Machine Learning Based Spherical Deconvolution for Intra-Voxel Fiber Estimation and Brain Connectivity Mapping

Tugba Tümer - 371244
Yagiz Gençer - 370462
Guillaume Noirot - 351691
École Polytechnique Fédérale de Lausanne, Switzerland

***Abstract*—Diffusion-weighted magnetic resonance imaging (DW-MRI) is a powerful imaging technique that relies on diffusion rate variations of water molecules in multiple directions to generate contrast in MR images. One common use of this technique is to visualize fibers in brain tissues, effectively revealing the neuronal wiring of the brain. In this project, we propose a novel approach for predicting the numbers, directions and volume fractions of fibers based on DW-MRI signals collected from different parts of the brain. Our work mainly consists of synthetic data generation, data augmentation for robustness, MLP model training, validation and optimization of the model, and finally testing the model on a real-world data unseen during the training and validation. At the end, the predictions of our model are also visualized as an alternative way of assessing its success.**

I. Introduction

DW-MRI capitalizes on the intrinsic diffusion properties of molecules to generate contrast in its images. Central to this technique is the Brownian motion of water molecules, which is influenced by the structural boundaries within biological tissues, such as membranes and fibers. By applying diffusion gradients in various directions and measuring the resultant signal intensities, DW-MRI enables the characterization of diffusion within each voxel—a volumetric pixel that represents a 3D unit of space in the imaging data.

The signal intensity in DW-MRI is inversely related to the degree of diffusion of water molecules along the direction of the applied gradient. Within a fiber, water molecules can move more freely parallel to the fiber direction, leading to a higher degree of diffusion and thus a reduced signal intensity. Conversely, diffusion is restricted perpendicular to the fiber direction, which results in a higher signal intensity. This anisotropic diffusion property is key to the utility of DW-MRI in capturing the orientation of fibers.

To infer detailed information about brain fibers, such as their paths and intersections, an effective model is imperative. The Diffusion Tensor Imaging (DTI) model [1] , which represents diffusion with a 3×3 tensor in each voxel, is a widely adopted approach due to its simplicity. However, DTI's limitations are pronounced in brain regions with intersecting fibers, as it can only model one principal diffusion direction.

High Angular Resolution Diffusion Imaging (HARDI) protocols have been developed to address the shortcomings of DTI. By sampling the diffusion signal across a larger number of gradient directions, HARDI captures complex angular information that DTI overlooks.

Among various HARDI-based techniques, Spherical Deconvolution (SD) stands out. SD provides estimates of the full fiber orientation distribution function (fODF) in each voxel, effectively resolving multiple fiber orientations [2]. This method assumes that the DW signal is a convolution of the response function, representing the signal from a single fiber population, with the fODF, indicative of the fiber density across orientations. However, the deconvolution process proved to be inherently ill-posed and sensitive to noise. To mitigate this, constraints are applied to the fODF reconstruction to prevent non-physical negative values [3].

II. Background and Dataset

The Signal Processing Laboratory 5 (LTS5) Diffusion Group focuses on brain tissue microstructure and structural connectivity –estimated by diffusion MRI data, with a particular focus on the reconstruction of the nerve fiber orientation distribution function (ODF) per voxel. This information is important for the reconstruction of the brain's white matter by using fiber tracking algorithms [4]. The group has implemented various novel reconstruction algorithms [5]–[7], and but now plans to develop a new generation of methods using machine learning techniques. In this project, we started to develop a machine learning pipeline for DW-MRI reconstruction under the supervisions of the laboratory director Prof. Jean-Philippe Thiran, Dr. Erick Jorge Canales-Rodríguez and PhD assistant Ekin Taskin.

This project is mainly inspired by HARDI (High Angular Resolution Diffusion Imaging) reconstruction challenge 2013, which was held in San Francisco (USA) in April 2013 as a part of the IEEE International Symposium on Biomedical Imaging (ISBI 2013) Conference [8]. Two members of the organizing committee were from EPFL, namely Assoc. Prof. Alessandro Daducci and the current director of LTS5, Prof. Jean-Philippe Thiran. The challenge was to develop a reconstruction method that reads the DW-MRI signal for each voxel and returns the corresponding number of fibers, their directions, and volume fractions in a predefined format. All the DW-MRI signals were given in the event website [9] with different noise levels (Signal to Noise Ratio (SNR) of 10, 20 and 30) as well as the ground-truth fiber information for competitors to test their successes. In this project, we decided to revisit the challenge ten years after the event. However, our idea was to reformulate the challenge as a machine learning problem, a relatively novel approach as this reconstruction problem has been almost exclusively tackled by more classical methods such as constrained spherical deconvolution (CSD) or linear programming.

III. Synthetic Data Generation

The HARDI dataset comes from a cube in 3-D space, each dimension having a length of 50 3-D pixels (voxels). This

makes in total $50 \times 50 \times 50 = 125000$ voxels. However, what we are interested in are the voxels in the white matter of the brain since it refers to the areas of the central nervous system (CNS) that are mainly made up of a large network of nerve fibers. When we apply the white matter mask to the dataset and extract only the voxels in the white matter, we end up with 13584 voxels.

Clearly, this number is not even remotely sufficient to train a neural network. Therefore, we needed a way to artifically generate signals that mimics the real data well enough and use them for training. We then split the real data into two, where the first part was used for validation and hyperparameter tuning and the second part was kept strictly for testing.

The HARDI dataset we use has 64 directions. This means each MRI signal S consists of 65 elements (the first element reserved for zero gradient case), where each element S_i(other than the first element) corresponds to one of the 64 unique predefined directions on a sphere, say (θ_i, ϕ_i). Then, the value of each element is given by:

$$S_i = S_{b=0} \times e^{-b \times D} \tag{1}$$

where $S_{b=0}$ is the signal intensity if the gradient intensity (b) were to be zero, b is the strength of the applied gradient in the direction (θ_i, ϕ_i), and D is the apparent diffusion coefficient (ADC) of the same direction. Our dataset has $b = 0$ for the first element and $b = 3000 s/mm^2$ for all the 64 directions. The actual directions (called b vectors) are also provided. From Eq.III, we see that the signal intensity in a direction with a higher diffusion intensity (D) is low and vice versa.

Moreover, it is known that water diffusivity is higher alongside a fiber than in the perpendicular directions. The diffusivity values (parallel diffusivity λ_1 and the diffusivities in the two perpendicular directions λ_2 and λ_3) and their ratios are critical for the task. Using the `response_from_mask_ssst()` function from the DIPY library [10], we estimated λ_1, λ_2 and λ_3, to be 0.00150 mm^2/s, 0.00039 mm^2/s and 0.00039 mm^2/s respectively.

In order to create synthetic signals (S_i's), we need to have a set of possible directions for fibers. For this, we first create 180 directions on a hemisphere as (θ_i, ϕ_i) pairs uniformly distributed between from 0° to 90° and from 0° to 360° respectively. We then call the `disperse_charges()` function from DIPY for 50000 iterations to update these directions such that they are distributed evenly on the hemisphere. The resulting possible synthetic fiber directions mapped on a hemisphere are given in Figure 2:

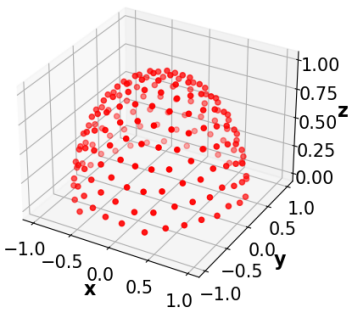

Figure 1: Synthetic Fiber Directions Mapped on a Hemisphere

DIPY library has a function called `multi_tensor()`, which for a voxel i returns its estimated DW-MRI signal S_i using its corresponding b values, b vectors, λ's, fiber directions in that voxel and their fractions. It also has an "snr" parameter that allows for signal creation with a given signal to Rician noise ratio, where Rician noise is the distribution of noise encountered in a typical DW-MRI signal. We first iterated over each of the 180 possible fiber directions and for each direction we created its corresponding signal assuming there exist a voxel with only a single fiber in that direction (with fraction 1). These responses are then collected in a matrix H of size 180x65, where each row holds the estimated signal of its corresponding signal found by `multi_tensor()` function.

However, one voxel might include more than one fiber, such that there are fiber crossings. Note that the signal response of a voxel that has multiple fibers with a given fraction distribution over its fibers is generally accepted to be the linear combination of their individual single-fiber responses combined by the same fraction distribution. Using this linearity, we follow the steps given below to create synthetic signals:

1) Decide the number of synthetic signals to be generated (N), each corresponding to one synthetic voxel.
2) For each synthetic signal to be created, randomly pick the number of fibers that it contains (N_f) - 1, 2 or 3 - either uniformly or with a given probability distribution.
3) Randomly select N_f number of indices of H to be combined as bases of the synthetic signal and N_f number of fractions such that they sum up to 1 and none of them is smaller than 0.10.
4) Linearly combine the selected base signals to create the synthetic signal.

The resulting signals to be used in training are collected as rows in a matrix S of size $N \times 65$. For each synthetic signal, the underlying indices of H and their linear combination fractions are stored in matrix F of size $N \times 180$ such that $F_{i,j}$ stores the linear combination coefficient of the jth row of H when constructing the i'th row of S. In other words:

$$S = FH \tag{2}$$

where each row i of F sums up to 1 and can be seen as the fiber orientation distribution function (fODF) of the signal in the i'th row of S. The main task of our model will be predicting the fODF corresponding to a signal input. Since each element of fODF is associated with one of the 180 directions, we can then deduce the fiber directions in the voxel that the input signal belongs to.

As a visual sanity check for our approach of mimicking the real data, we select a real signal from the validation set and read its ground truth peaks and directions. It has two fibers with angles $(\theta, \phi) = (62.4, -175.8)$ and $(50.5, -175.5)$ with fractions 0.76 and 0.24 respectively. We then generate its synthetic approximate using the above-given approach and plot the signals on top of each other to compare them. The result is given in Figure 2:

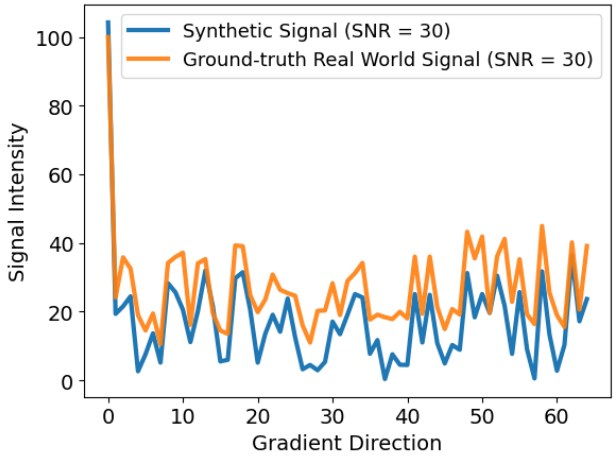

Figure 2: A Real Signal and Its Synthetic Approximate

Here, we verify that our synthetic data has the same trend of its ground-truth at all points and resembles it very closely. After inspecting many such samples, we decide that our synthetic dataset can be used in training and the resulting model should perform well when tested by real data.

IV. Model Training and Validation

In this project, we choose fully connected MLP as our architecture implemented in PyTorch. For the validation, we first detect the peaks of returned F using `detect_peaks()` function in `helpers.py`, which utilizes DIPY's `peak_directions()` function to extract the peaks and puts the results in the same format as HARDI dataset's ground-truths. Then, we have a script called `compute_local_metrics.py`, which returns our prediction's error in terms of its percentage error in detected number of peaks, angular error of fiber orientations and error in their fractions. This is done by first pairing the predicted fibers with the ground-truth fibers based on their directions. Then, the angular and fractional errors coming from each pair are added up to give the angular and fractional error of the voxel respectively. If the number of predicted fibers is different than the ground-truth number, for each fiber that is unpaired an angle error of 45°and the fraction of the fiber are directly added to the voxel's total angular error and fractional error respectively.

We first began with training a model with 100,000 synthetic signals (voxels), the number of fibers to be contained in each voxel were selected uniformly at random, layer sizes were $(512, 256, 128)$, the loss function used was the MSE between the ground-truth ODF (F) vs. the predicted (output) F. The activation function used was ReLU and the learning rate was 0.001. The results were quite poor, as the mean (averaged over all the voxels) percentage error in number of fibers was 283% and the mean angular error was 45.3%.

We then started using batch normalization at each hidden layer. Furthermore, instead of choosing the number of fibers (Nf) in voxels uniformly at random, we began to use a custom probability distribution that puts more emphasis on the single-fiber voxels as they are present in the real-world more often.

We also incorporated data augmentation for robustness against Rician noise. Here, we first create the synthetic signals as before. Then, each signal is recreated multiple times but with different noise levels (e.g. SNR = 10, 20, 30 and noiseless), although the ground-truth ODF stays the same. The aim here is to teach our model that a DW-MRI signal refers to the same ODF even though it carries different instances of noise.

Another try was to include S loss to the training loss. Note that given a set of signals S, we try to find F_{pred} such that $S \approx S_{pred} = F_{pred}H$. In order to achieve better angle predictions we have in some models S and F MSE losses together. In such cases the used loss is $MSE(S,S_{pred}) + 5000 \times MSE(F, F_{pred})$ to bring the two into comparable values. Some of the trained models with their validation results is given in Table I:

Data Size	Layers	Loss	SNR's	PNPE	AE	FE
6e5	512, 256, 128	F	10:30:10	24.0%	33.0°	0.377
6e5	512, 256, 128	F	10:30:2.5	77.2%	28.2°	0.574
1.2e6	1024, 512, 256	F	10:30:5	31.7%	29.1°	0.444
1.2e6	512, 256, 128	F	10:30:5	23.2%	34.0°	0.258
3e5	512, 256, 128	F	10:30:5	38.6%	29.9°	0.367
3e5	65, 128, 180	F	10:30:5	28.8%	33.6°	0.263
6e5	128, 256, 256, 128	F	10:30:5	35.3%	28.1°	0.516
6e5	512, 256, 128	F	10:30:5	27.4%	26.5°	0.356
6e5	64, 128, 256	F	10:30:5	37.9%	31.4°	0.438
6e5	512, 256, 128	S+F	10:30:5	29.7%	25.5°	0.304
6e5	512, 256, 128	S+F	20:30:10	15.3%	32.2°	0.196
6e5	65, 128, 180	S+F	20:30:10	39.5%	33.6°	0.519
1.2e6	256, 256, 256	S+F	20:30:5	26.6%	30.6°	0.460
1.2e6	512, 512	S+F	20:30:5	281.4%	35.3°	0.950

Table I: Validation Results with Different Parameters

The notation x:y:z in the SNR's column means that the data is augmented with noises from SNR = x to y with z increments. PNPE, AE and FE means Peak Number Percentage Error, Angular Error, and Fraction Error respectively, each of them being the average error over all the validation voxels. We also briefly tried incorporating weight decay (L_2 normalization) and increasing the learning rate by changing the learning rate of the model in the 8^{th} row of Table I to 0.01 and adding weight decay to the model in the 10^{th} row. However, we observed an increases of about 15% in PNPE and 2% in AE and therefore did not pursue these approaches further. Note that these calculations are made with the data with SNR = 30.

V. Test Results

The main objective is to keep all three errors simultaneously small but with a special emphasis on the angular error. Therefore, our best model is given in the 10^{th} row of Table I with a total voxel angular error of 25.5°on average. The visual representation of our final architecture is given in Figure 3:

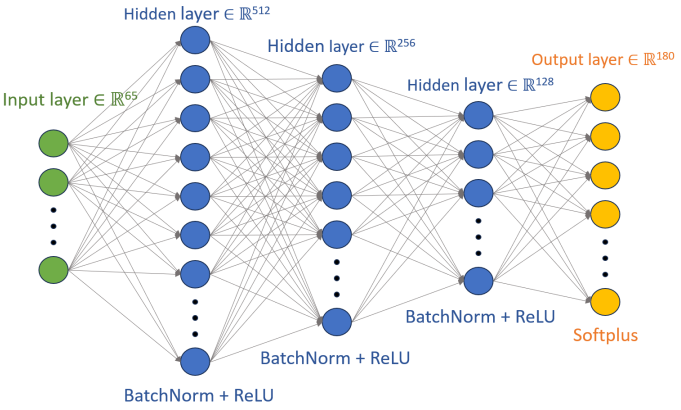

Figure 3: Final MLP Architecture

The validation errors of our final architecture were given in the 10^{th} row of Table I as stated before. We now calculate the metrics again using the test set we saved from the HARDI dataset, which remained unseen during training and validations steps. We see that it achieves PNPE, AE, and FE errors of 29.8%, 25.1°and 0.302 respectively. It is not surprising that these values are very close to the validation values as the training was achieved by using only synthetic data.

Now, we want to test the success of our model on a real-world data and visualize the results. In Figure 4 you can see the visualization of two different voxels. In each voxel, the left one is the ground-truth and the right one is our model's prediction.

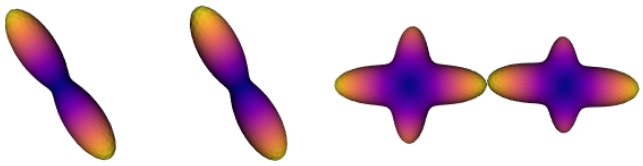

(a) Voxel with single fiber (b) Voxel with two fibers

Figure 4: Visualization of the real-world voxels where the left signal is ground truth and the right one is predicted

For a better visualization, we also want to take a slice from the 3-D space and visualize all the ground-truth fibers and our predictions on that place and compare the results. This is done in Figure 5:

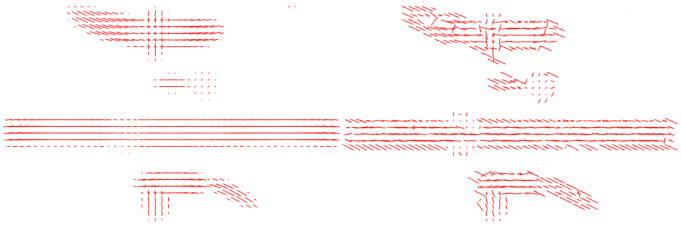

(a) Ground-Truth Peaks (b) Predicted Peaks

Figure 5: Visualization of the real-world data slice

Looking at the visual comparisons, we see that although far from perfect, our model manages to predict the general direction or 'trend' of the fiber orientations in the white-matter of the brain reasonably well. Furthermore, it is important to note that the parts with fibers (red parts) in Figure 5 correspond to the white matter regions of the slice. Our predictions are considerably worse at the edges of this region, which is a sensible result as our model is trained to predict the fiber distributions for the pure white-matter regions.

VI. Discussion and Comments

In this project, we made use of a relatively simple type of neural network, namely an MLP architecture. However, we believe that the importance of our work mainly lies in the various original approaches we employed in synthetic data creation, it's augmentation with different noise levels, creating metrics the train loss and DW-MRI error calculations, etc. As stated before, machine learning based approaches are still rare in the subject of DW-MRI reconstruction. This made it imperative for us to experiment with novel ideas and come up with our solutions.

The main weaknesses of our approach was that we had to rely on synthetic data generation which, although conducted with care, might have led to sub-optimal results. Furthermore, we disregarded the spacial dependency of the fiber distributions, which normally offers significant information as the closer fibers are generally more likely to have similar orientations. This information can be integrated in future by the use of architectures that take spacial correlations into the account, such as Convolutional Neural Networks.

At the end, it was a pleasure for us to work on this project and we hope that further development of machine learning based DW-MRI reconstruction algorithms will pave the road for better diagnosis in the medical field.

Acknowledgements

We thank the Signal Processing Laboratory 5 (LTS5), especially our project supervisors Dr. Erick Jorge Canales-Rodríguez and Ekin Taskin for their valuable help and support.

VII. Ethical Risks

Our project's primary use is in medical domain, which further amplifies the importance of ethical risk evaluation. We can categorize the potential stakeholders into two main categories, namely the patients from which the data is collected from and researchers that can potentially utilize our synthetic data or model for further studies. The main indirect stakeholders are the medical professionals that could use our model in the future and the environment. Our project's primary ethical concern stems from the potential bias inherent in the dataset used to train our model.

Ethical risks that might be related to patients are related with their potentially sensitive data and the risk of using a skewed dataset such that the trained model would turn out to be applicable for a highly specific group of people. The first risk is avoided in our project as the HARDI dataset used does not include any personal information other than the DW-MRI signal itself. The second risk is mitigated by the use of synthetic data for the training which utilizes a very broad procedure, making it very hard to overfit to any special subset of population. However, the validation dataset used to optimize the model hyperparameters can be extended in the future, ensuring that the model performs well for all groups of people. The ethical risks related to researchers are substantially mitigated by our extensive explanation of the project pipeline and the fact that our codebase is open source on GitHub. Still, we encourage all the researchers to not just rely on our statements but to test and reproduce our findings and assess its applicability to their specific research. This is also true for medical professionals as indirect stakeholders since the model must be tested and verified before it can be trusted as a medical tool. Last but not least, the carbon footprint of training a neural network is often a critical concern. Although we could not completely overcome

the issue, we reduced its effect by training an MLP model rather than more advanced architectures and used fairly small number of parameters. Furthermore, we did not employ an exhaustive grid search for the validation but instead were more selective in deciding the values of hyperparameters to try out, effectively reducing our negative impact on the environment.

REFERENCES

[1] P. Basser, J. Mattiello, and D. Lebihan, "Estimation of the effective self-diffusion tensor from the nmr spin echo," *Journal of Magnetic Resonance, Series B*, vol. 103, no. 3, pp. 247–254, 1994. [Online]. Available: https://www.sciencedirect.com/science/article/pii/S1064186684710375

[2] J.-D. Tournier, F. Calamante, D. G. Gadian, and A. Connelly, "Direct estimation of the fiber orientation density function from diffusion-weighted mri data using spherical deconvolution," *NeuroImage*, vol. 23, no. 3, pp. 1176–1185, 2004. [Online]. Available: https://www.sciencedirect.com/science/article/pii/S1053811904004100

[3] J.-D. Tournier, F. Calamante, and A. Connelly, "Robust determination of the fibre orientation distribution in diffusion mri: Non-negativity constrained super-resolved spherical deconvolution," *NeuroImage*, vol. 35, no. 4, pp. 1459–1472, 2007. [Online]. Available: https://www.sciencedirect.com/science/article/pii/S1053811907001243

[4] G. Girard, K. Whittingstall, R. Deriche, and M. Descoteaux, "Towards quantitative connectivity analysis: reducing tractography biases," *NeuroImage*, vol. 98, pp. 266–278, 2014. [Online]. Available: https://www.sciencedirect.com/science/article/pii/S1053811914003541

[5] E. J. Canales-Rodríguez, A. Daducci, S. N. Sotiropoulos, E. Caruyer, S. Aja-Fernández, J. Radua, J. M. Yurramendi Mendizabal, Y. Iturria-Medina, L. Melie-García, Y. Alemán-Gómez, J.-P. Thiran, S. Sarró, E. Pomarol-Clotet, and R. Salvador, "Spherical deconvolution of multichannel diffusion mri data with non-gaussian noise models and spatial regularization," *PLOS ONE*, vol. 10, no. 10, pp. 1–29, 10 2015. [Online]. Available: https://doi.org/10.1371/journal.pone.0138910

[6] E. J. Canales-Rodríguez, J. H. Legarreta, M. Pizzolato, G. Rensonnet, G. Girard, J. Rafael-Patino, M. Barakovic, D. Romascano, Y. Alemán-Gómez, J. Radua, E. Pomarol-Clotet, R. Salvador, J.-P. Thiran, and A. Daducci, "Sparse wars: A survey and comparative study of spherical deconvolution algorithms for diffusion mri," *NeuroImage*, vol. 184, pp. 140–160, 2019. [Online]. Available: https://www.sciencedirect.com/science/article/pii/S1053811918307699

[7] E. Canales-Rodríguez, L. Melie-Garcia, and Y. Iturria, "Mathematical description of q-space in spherical coordinates: Exact q-ball imaging," *Magnetic resonance in medicine : official journal of the Society of Magnetic Resonance in Medicine / Society of Magnetic Resonance in Medicine*, vol. 61, pp. 1350–67, 06 2009.

[8] "Hardi reconstruction challenge 2013," http://hardi.epfl.ch/static/events/2013_ISBI/,.

[9] "Testing data," http://hardi.epfl.ch/static/events/2013_ISBI/testing_data.html#classical-sampling-schemes,.

[10] "Diffusion imaging in python (dipy) documentation," https://docs.dipy.org/stable/index.html,.